THE JOURNAL OF PHYSICAL CHEMISTRY A

Article

pubs.acs.org/JPCA

Theoretical Study on the Microhydration of Atmospherically Important Carbonyl Sulfide in Its Neutral and Anionic Forms: Bridging the Gap between the Bulk and Finite Size Microhydrated Cluster

Saptarsi Mondal, Avula Uday Teja, and Prashant Chandra Singh*

Department of Spectroscopy, Indian Association for the Cultivation of Science, Kolkata 700032, India

Supporting Information

ABSTRACT: Carbonyl sulfide (OCS) is the most abundant and stable sulfur-containing triatomic gas present in the atmosphere that plays an important role in aerosol formation. Structure, energetics, and photoelectron spectral properties of the microhydrated OCS in its neutral and anionic forms have been studied by using the BP86, B3LYP, and MP2 methods. OCS is linear in the neutral state but bent in the anionic state. Water binds with the OCS through a single hydrogen bond (O−H···O) in the OCS-$(H_2O)_n$ [n = 1−6], whereas binding of OCS^- with water takes place through single as well as double hydrogen bonds (O−H···S and O−H···O). Energy decomposition analysis shows that electrostatic and exchange energies are the main contributors to the stabilization energy of the microhydrated OCS and OCS^- clusters. Detachment as well as solvation energies are calculated with different levels of theory and compared with the existing experimental values. Finally, an analytical expression has been used to obtain the bulk value of the detachment and solvation energies from the existing information on the finite size clusters. The present study reveals that hydration increases the detachment energy of the OCS^- by 3.2 eV. In the absence of experimental bulk values of the detachment and solvation energies for this system, the values obtained by the solvent-number-dependent theoretical expression will definitely reduce this gap and may be used for the modeling of the OCS in the atmosphere.

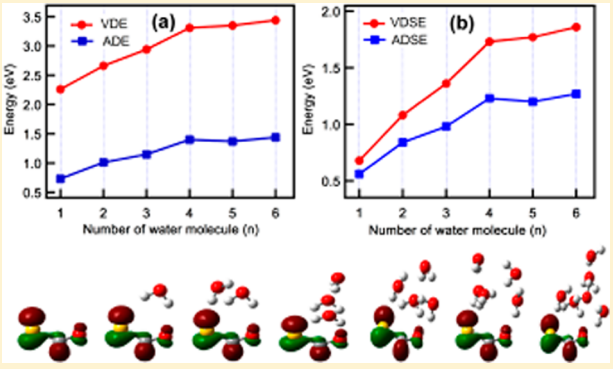

INTRODUCTION

Carbonyl sulfide (OCS), an efficient greenhouse gas, is the most abundant and stable sulfur-containing triatomic gas in the atmosphere and plays a significant role in the global sulfur cycle.[1] OCS is nearly chemically inert in the troposphere, and most of it is transported into the stratosphere where it plays an important role in the formation of the aerosol through various chemical processes.[1−3] The aerosol formation affects the earth's radiation balance and its climate. Various experimental and theoretical studies have been performed to decipher the chemistry of OCS in atmospheric conditions.[2−4] OCS produces sulfur-containing compounds in the stratosphere either by photolysis or reaction with OH and O radicals, which further assist in the aerosol formation. It has been shown that the hydrolysis of OCS depends on the water content and relative humidity, which suggests that the water clusters of OCS play an important role in the aerosol formation.[5,6] The structure and energetic aspect of hydrated OCS up to four water molecules has been discussed in the literature by various groups.[4,6−8]

In contrast to the OCS neutral molecule, its anion (OCS^-) is a metastable species. Indeed, in one of the mass spectroscopic studies, OCS^- was not observed on the photodissociation of OCS, which was attributed to its nonexistent adiabatic electron affinity.[9] However, in the same experimental study, the hydrated cluster of OCS^-, including, in particular, monohydrated OCS^- along with larger cluster ions, was produced readily and in abundance.[10,11] The existence of mono and other higher hydrated anions indicates that OCS^- is stabilized by hydration. The photoelectron study of the OCS^- provided the vertical detachment energy (VDE) of the mono and dihydrated clusters, which infers about the nature of hydrogen bonding between the water and OCS^-.[10] Stepwise hydration of a particular system provides insight information about the nature of intermolecular interaction between the solute and water molecules.[12−22] The main structural difference between the two states of the OCS is that it is linear in the neutral form but bent in its anionic state. It will be interesting to understand the nature of intermolecular interaction, energetics, solvation, and detachment energies of the OCS in neutral and anionic forms with water during the stepwise hydration.

In this paper, we have performed a detailed and systematic theoretical study on the structure and energetics of the

Received: February 17, 2015
Revised: March 25, 2015
Published: March 25, 2015

DOI: 10.1021/acs.jpca.5b01638
J. Phys. Chem. A 2015, 119, 3644−3652

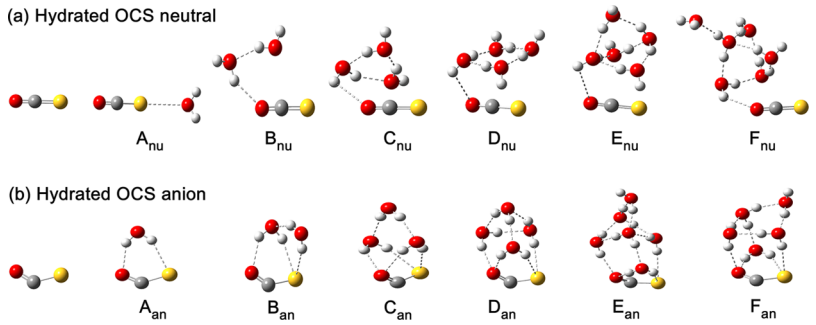

Figure 1. (a) Optimized minimum-energy structures of OCS neutral and OCS-$(H_2O)_n$ [n = 1−6] (A_{nu}−F_{nu}), (b) optimized minimum-energy structures of OCS^- and OCS^--$(H_2O)_n$ [n = 1−6] (A_{an}−F_{an}) obtained at the MP2/6-311++G(d,p) level of theory. Oxygen, hydrogen, carbon, and sulfur atoms are depicted in red, white, black, and yellow, respectively. A−F denote the structures with an increasing number of water molecules starting from one to six.

microhydrated OCS (up to six water molecules) in its neutral and anionic forms. All of the structures have been optimized at the B3LYP, BP86, and MP2 methods with the 6-311++G(d,p) basis set. Further, we have calculated the detachment and solvation energies of the microhydrated OCS^-, and the values obtained are compared with the existing experimental values. The computational cost for the calculation of solvation and detachment energies of OCS^- increases tremendously with the increase of the water molecules, and it becomes almost an impossible task to calculate the bulk solvation and detachment energies by using the same method. In this work, solvent-number-dependent analytical expressions have been used to obtained the bulk solvation and detachment energies of the OCS^-.

METHODOLOGY

All of the structures of the neutral and anionic OCS monomer along with its hydrated clusters have been obtained by the optimization at the BP86, B3LYP, and MP2 levels of theory with the 6-311++G(d,p) basis set. Several initial structures have been designed based on the chemical intuitions, and the optimization of these structures has been performed to find the minimum-energy structure. The most important concern in this process is to guess a good initial structure that can easily converge to a local or global minimum. Initial guess structures have been first optimized with the HF/6-31+G(d) level of theory, and the optimized structures obtained from this calculation have been used as an initial structure for the optimization at the BP86, B3LYP, and MP2 methods. The initial structures for larger size clusters were prepared with the bottoms-up approach based on the structures of smaller clusters. For example, in order to find the possibility of the maximum number of minimum-energy structures of the dihydrated OCS, we have first taken the most stable structure of monohydrated OCS followed by the addition of subsequent water to all possible binding sites, and the same procedure was followed with the other stable structures of the monohydrated OCS. However, by this approach, there is a chance that the most stable structure can be missed on the potential energy surface. Hence, a few initial structures were also designed systematically following by a top-down approach to determine the most stable one. Neutral clusters have been optimized with the restricted approach, whereas the unrestricted optimization method was applied for the anionic clusters. Harmonic frequency calculation was performed for all of the structures in order to confirm the nature of the optimized structures. The positive frequencies were obtained for all of the hydrated clusters of both neutral and anionic OCS along with its monomer, confirming that a particular structure is a minimum-energy structure. The values of the spin contamination $\langle S^2 \rangle$ were found to be ∼0.768 for the unrestricted calculation of the OCS^- and its hydrated clusters, which are quite close to the acceptable value of 0.75 for the pure doublet system. The stabilization energy of the system has been corrected for the basis set superposition position error (BSSE) and the zero-point vibrational energy (ZPE) correction. BSSE calculation has been performed by the counterpoise correction method. All of the above calculations have been performed by the Gaussian 09 suite of programs.[23] Furthermore, the stabilization energy of the microhydrated OCS and OCS^- clusters has been decomposed into electrostatic, exchange, polarization, dispersion, and repulsion energies by using the energy decomposition scheme local molecular orbital energy decomposition analysis (LMOEDA) incorporated into the GAMESS software.[24]

RESULT AND DISCUSSION

(a). Structure and Energetics. A number of stable minimum-energy structures of microhydrated neutral OCS as well as its anion were obtained by the optimization process using the BP86, B3LYP, and MP2 methods with the 6-311++G(d,p) basis set. Figure 1 depicts the minimum-energy structures of the microhydrated OCS (A_{nu}−F_{nu}) and OCS^- (A_{an}−F_{an}) clusters along with their respective monomers obtained at the MP2/6-311++G(d,p) level of theory. BP86 and B3LYP levels of theory provide the same structures of the microhydrated OCS and OCS^-. OCS is a linear molecule, whereas OCS^- has a bent structure. For monohydrated OCS, water interacts with the sulfur of the OCS moiety (O−H···S). The reported structure of the monohydrated OCS is in accordance with the experimentally obtained structure by Tatamitani and Ogata.[6−8] For higher-order clusters of microhydrated OCS, the first water molecule forms a hydrogen bond with the oxygen of the OCS moiety, and other water molecules form an intermolecular hydrogen bond (IHB) with the first water molecule [B_{nu}−F_{nu}]. In contrast to the monohydrated OCS, its monohydrated anion has an asymmetric double hydrogen-bonded (DHB) arrangement of water in which both of the OH groups of the water molecule are donors and hydrogen-bonded to oxygen (O−H···O) and sulfur (O−H···S) of the OCS^-. An asymmetric DHB structure of the monohydrated OCS^- has also been obtained experimentally

DOI: 10.1021/acs.jpca.5b01638
J. Phys. Chem. A 2015, 119, 3644−3652

Table 1. Stabilization Energy (kcal/mol) of OCS-$(H_2O)_n$ and OCS^--$(H_2O)_n$ [n = 1−6] Calculated at the BP86, B3LYP, and MP2 Methods with the 6-311++G (d,p) Basis Set[a]

	OCS-$(H_2O)_{n=1-6}$					
	A_{nu}	B_{nu}	C_{nu}	D_{nu}	E_{nu}	F_{nu}
BP86	1.3, *0.8*, (0.2)	7.4, *6.1*, (3.0)	16.4, *14.9*, (10.7)	25.4, *22.1*, (14.2)	38.4, *33.1*, (22.0)	46.5, *40.3*, (26.8)
B3LYP	1.5, *1.1*, (0.4)	8.6, *7.4*, (4.2)	18.9, *16.7*, (11.2)	24.3, *21.1*, (16.6)	39.7, *35.0*, (23.2)	48.9, *40.5*, (26.8)
MP2	2.2, *1.3*, (0.5)	10.7, *7.1*, (3.8)	21.7, *14.8*, (10.1)	29.9, *21.5*, (13.6)	43.6, *30.2*, (19.2)	51.0, *37.8*, (24.1)
	OCS^--$(H_2O)_{n=1-6}$					
	A_{an}	B_{an}	C_{an}	D_{an}	E_{an}	F_{an}
BP86	14.2, *13.3*, (11.3)	26.6, *24.5*, (20.3)	37.6, *34.6*, (28.2)	51.9, *47.6*, (37.5)	64.6, *58.7*, (46.2)	74.8, *68.0*, (54.1)
B3LYP	14.0, *13.2*, (11.0)	26.0, *24.2*, (19.8)	37.5, *34.8*, (27.1)	51.0, *47.2*, (36.8)	63.3, *58.1*, (45.0)	73.6, *67.6*, (51.5)
MP2	15.2, *12.5*, (10.4)	28.3, *22.5*, (17.9)	42.0, *33.2*, (25.5)	55.6, *43.7*, (33.3)	68.5, *53.0*, (40.6)	79.8, *61.7*, (45.9)

[a]BSSE-corrected energies (kcal/mol) are depicted in italics, and the values shown in the parentheses (kcal/mol) correspond to the BSSE as well as ZPE-corrected values at the respective levels of theory.

by Johnson and co-workers.[16] Dihydrated OCS^- (B_{an}) has one water that is DHB to OCS^-, and the other water molecule is intermolecular hydrogen bonded to the first water molecule as well as being hydrogen-bonded to the sulfur terminal of the OCS^-. The most stable structures of other higher hydrated clusters of the OCS^- (C_{an}−F_{an}) depict that OCS^- is always at the surface and that growth of a water network takes place either at the top or bottom. Growth of the water network around the OCS^- comprises both an IHB as well as ion−water hydrogen bonding. It has been observed that a maximum of four water molecules can directly interact with the OCS^- through a single or double hydrogen bond, which indicates that the primary solvation shell of the OCS^- may have four water molecules.

Table 1 depicts the value of stabilization energy of microhydrated OCS and OCS^- clusters calculated at the BP86, B3LYP, and MP2 levels of theory with the 6-311++G(d,p) basis set. The value of the stabilization energy for the microhydrated OCS and OCS^- clusters increases with an increase of the number of water molecules. The trend of the stabilization energy obtained from all levels of theory is the same for microhydrated OCS and OCS^-. Figure 2 shows the change in the stabilization energy of microhydrated OCS and OCS^- clusters with respect to the number of water molecules in the particular cluster at the MP2 level of calculation. It is clearly observed that the stabilization energy varies linearly with the number of water molecules for both systems. However, the stabilization energy for the microhydrated OCS^- clusters is higher as compared to the neutral OCS. A similar trend of data has been found for the B3LYP and BP86 levels of calculation. The stabilization energy data for microhydrated OCS and OCS^- (Figure 2) has been fitted with a linear equation, and the slopes of the lines have been found to be 9.5 and 12.6 for the microhydrated neutral and anion OCS clusters, respectively. The slope of the line indicates that the average stabilization energy increases by 9.5 kcal/mol for microhydrated neutral OCS clusters, whereas it increases by 12.6 kcal/mol for microhydrated OCS^- with the addition of successive water molecules. Table 1 also shows the BSSE- and ZPE-corrected stabilization energy at the respective levels of theory, which depicts that these corrections only decrease the complexation energy but do not change the trend. The amount of BSSE for the MP2 level of theory is higher as compared to that for the BP86 and B3LYP methods.

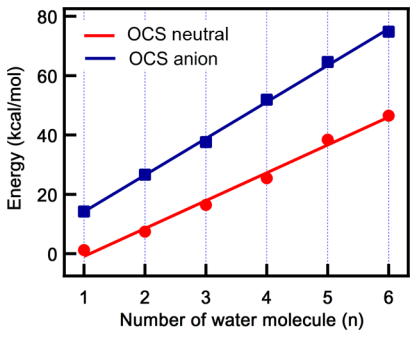

Figure 2. Plot of the stabilization energy with respect to the number of water molecules (n) in the OCS-$(H_2O)_n$ (red circle) and OCS^--$(H_2O)_n$ (blue square) clusters calculated at the MP2/6-311++G(d,p) level of theory. The red and blue lines represent the linear fit for the OCS-$(H_2O)_n$ and OCS^--$(H_2O)_n$ systems, respectively. The value of the correlation coefficient was found to be 0.99, which reflects high reliability of the fitting.

In order to get insight on the stabilization energy of the microhydrated OCS and OCS^-, it was further decomposed into electrostatic, exchange, polarization, dispersion, and repulsion energies by using the energy decomposition scheme LMOEDA incorporated in the GAMESS.[24] Table 2 shows the contribution of different energy components of the microhydrated OCS and OCS^- obtained at the MP2 and B3LYP levels of theory. Energy components at the MP2 and B3LYP levels of theory follow the similar trend however; absolute values of the exchange and dispersion energies are comparatively higher for the MP2 level of theory. The values of the electrostatic and exchange energies for the microhydrated OCS^- are higher compared to those for the microhydrated OCS due to which net stabilization energy is higher for the microhydrated OCS^-. It can be seen that the electrostatic and exchange energies are the main contributors to the stabilization energy of the microhydrated OCS and OCS^- clusters. The stabilization energy contributed by the electrostatic, exchange, polarization, and dispersion energies outweighs the destabilization energy provided by the repulsion energy.

The total and incremental association energies of the hydrated clusters are other important energy parameters that have been used to discuss the energetics of many hydrated anionic and neutral systems.[25−28] The total association energy depicts the available energy on the binding of the molecules to the water cluster, whereas the incremental association energy provides the energetics of the loss of a water molecule from a given cluster to form the $(n - 1)$ clusters.

DOI: 10.1021/acs.jpca.5b01638
J. Phys. Chem. A 2015, 119, 3644−3652

Table 2. Decomposition of the Total Stabilization Energy into the Electrostatic (E_{elec}), Exchange (E_{exc}), Polarization (E_{pol}), Dispersion (E_{disp}), and Repulsion (E_{rep}) in kcal/mol for the OCS-$(H_2O)_n$ as Well as OCS^--$(H_2O)_n$ [n = 1−6], Respectively Calculated at the MP2 and B3LYP Methods with the 6-311++G(d,p) Basis Set[a]

	E_{elec}	E_{exc}	E_{pol}	E_{disp}	E_{rep}
			OCS-$(H_2O)_{n=1-6}$		
A_{nu}	−2.7 (−2.4)	−2.8 (−0.8)	−0.7 (−0.9)	−0.2 (−1.3)	5.0 (4.0)
B_{nu}	−15.0 (−14.1)	−16.8 (−5.78)	−4.2 (−5.46)	−0.7 (−5.27)	29.6 (23.1)
C_{nu}	−30.9 (−31.6)	−36.8 (−14.9)	−9.6 (−13.9)	−2.6 (−6.4)	65.5 (52.8)
D_{nu}	−40.3 (−39.9)	−46.1 (−18.2)	−12.3 (−17.1)	−3.1 (−12.3)	82.4 (66.1)
E_{nu}	−66.2 (−65.8)	−81.9 (−33.9)	−25.5 (−34.3)	−5.5 (−18.5)	147.8 (117.9)
F_{nu}	−76.8 (−77.0)	−91.7 (−38.6)	−28.5 (−37.0)	−5.8 (−23.8)	165.8 (137.2)
			OCS^--$(H_2O)_{n=1-6}$		
A_{an}	−20.9 (−19.6)	−17.8 (−7.7)	−4.5 (−5.4)	−0.2 (−4.2)	30.8 (23.2)
B_{an}	−38.8 (−36.9)	−35.7 (−16.3)	−9.0 (−14.8)	−1.1 (−8.1)	61.7 (51.2)
C_{an}	−60.0 (−60.1)	−58.9 (−27.6)	−15.2 (−20.6)	−2.0 (−14.1)	102.8 (85.5)
D_{an}	−77.8 (−77.1)	−76.1 (−34.0)	−20.7 (−27.5)	−3.3 (−18.9)	133.8 (109.4)
E_{an}	−96.3 (−96.8)	−101.0 (−46.2)	−30.6 (−40.6)	−4.9 (−23.7)	179.0 (147.8)
F_{an}	−113.3 (−114.0)	−119.6 (−53.4)	−37.0 (−48.3)	−5.9 (−29.3)	213.1 (175.7)

[a]The values depicted in parentheses correspond to the B3LYP level of calculation.

Table 3. Total and Incremental Association Energy (kcal/mol) for the OCS^--$(H_2O)_n$ [n = 1−6] Calculated at the BP86, B3LYP, and MP2 Methods with the 6-311++G(d,p) Basis Set[a]

		total association energy		incremental association energy	
	methods	ΔE_e	ΔE_0	ΔE_e	ΔE_0
2w	BP86	24.9 (23.7)	24.1 (22.9)	12.4 (11.2)	10.2 (9.1)
	B3LYP	24.1 (23.1)	23.5 (22.5)	12.0 (10.9)	9.8 (8.8)
	MP2	8.9 (4.7)	8.1 (3.9)	12.2 (9.9)	10.5 (7.3)
3w	BP86	27.1 (26.4)	26.4 (25.7)	13.1 (12.2)	9.7 (8.8)
	B3LYP	26.2 (25.4)	25.4 (24.6)	12.7 (12.0)	9.4 (8.6)
	MP2	11.7 (6.9)	10.7 (6.0)	14.5 (10.6)	11.1 (8.3)
4w	BP86	34.0 (32.6)	33.1 (31.7)	12.1 (10.9)	9.5 (8.3)
	B3LYP	32.7 (31.6)	31.8 (30.7)	12.2 (11.0)	9.5 (8.4)
	MP2	13.6 (8.8)	12.9 (8.1)	13.6 (8.5)	10.9 (6.9)
5w	BP86	34.1 (32.7)	33.5 (32.6)	12.3 (11.1)	9.9 (8.6)
	B3LYP	33.3 (32.3)	32.3 (31.4)	12.1 (10.9)	9.5 (8.2)
	MP2	19.3 (13.1)	17.5 (11.5)	13.8 (11.4)	9.8 (7.4)
6w	BP86	34.9 (33.9)	34.3 (33.2)	10.5 (9.3)	7.6 (6.4)
	B3LYP	33.9 (32.9)	32.5 (31.6)	10.5 (9.8)	7.5 (6.5)
	MP2	20.7 (14.5)	19.2 (13.1)	11.2 (8.0)	8.8 (5.6)

[a]ΔE_e corresponds to the electronic energy values, and the values given in the parentheses for this column depict the BSSE-corrected values. ΔE_0 shows the ZPE-corrected values, and the values given in the parentheses for this column correspond to the BSSE- as well as ZPE-corrected values of the energies.

$$OCS + (H_2O)_n + e^- \rightarrow OCS^-(H_2O)_n \quad (1)$$

$$OCS^-(H_2O)_{n-1} + H_2O \rightarrow OCS^-(H_2O)_n \quad (2)$$

The total association energy has been calculated by using the energy values of the species shown in eq 1, whereas the incremental association energy has been calculated by using eq 2. The values of the total and incremental association energies for n = 2−6 clusters have been calculated by using the BP86, B3LYP, and MP2 methods, and the values are shown in Table 3. The values of the total association energy obtained at the MP2 level of theory are less as compared to those for B3LYP and BP86. The total association energy increases up to the four water molecules and then becomes almost constant for all of the levels of calculation. This may be attributed to the completion of the first hydration shell of the OCS^- with four water molecules. The incremental association energy depicts that the addition of each water molecule increases the stabilization energy by ∼10 kcal/mol. BSSE- and ZPE-corrected values of the total and incremental association energies are also listed in Table 3, which depicts that these corrections only decrease the values of the total and incremental association energy, and the trend of the data remains the same. The BSSE corrections with the B3LYP and BP86 methods are much smaller than the ones at the MP2 level for the total association energy, and a similar trend is also followed for the incremental association energy.

(b). Vertical and Adiabatic Detachment Energies. The VDE accounts for the energy required to remove the electron when the structure of the neutral species is fixed at the equilibrium geometry of its anion, whereas the adiabatic electron affinity (ADE) describes the minimum energy required to remove an electron when the neutral species relaxes to its equilibrium geometry. The ADE [$E_{ADE}(n)$] and VDE [$E_{VDE}(n)$] of the OCS^--$(H_2O)_n$ clusters have been calculated in the following way

DOI: 10.1021/acs.jpca.5b01638
J. Phys. Chem. A 2015, 119, 3644−3652

Table 4. VDE and ADE (eV) for the OCS^--$(H_2O)_n$ [n = 1−6] Calculated at the BP86, B3LYP, MP2, and CCSD(T) Methods with the 6-311++G(d,p) Basis Set

	VDE (eV)					ADE (eV)			
	BP86	B3LYP	MP2	CCSD(T)	Exp	BP86	B3LYP	MP2	CCSD(T)
A_{an}	2.26	2.33	1.56	1.72	2.07 ± 0.07	0.73	0.69	−0.02	0.21
B_{an}	2.66	2.69	2.03	2.18	2.53 ± 0.07	1.01	0.92	0.18	0.41
C_{an}	2.94	2.99	2.26	2.41		1.15	1.08	0.34	0.58
D_{an}	3.31	3.34	2.59	2.75		1.40	1.32	0.62	0.86
E_{an}	3.35	3.37	2.64	2.78		1.37	1.27	0.56	0.74
F_{an}	3.44	3.46	2.74	2.89		1.44	1.37	0.66	0.91

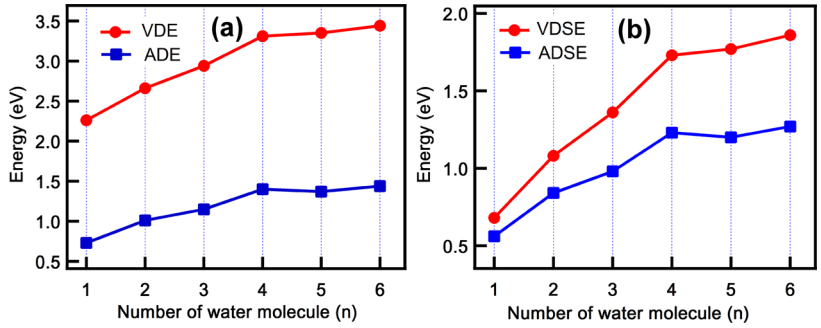

Figure 3. Plots of the VDE (red) and ADE (blue) (a) and (b) solvation energies with respect to the number of the water molecules, respectively, obtained at the BP86/6-311++G(d,p) level of calculation. Red and blue lines in both plots are eye guide lines for the change of the respective data.

$$E_{VDE}(n) = [E_s(OCS\text{-}nH_2O) - E(OCS^-\text{-}nH_2O)]$$

$$E_{ADE}(n) = [E(OCS\text{-}nH_2O) - E(OCS^-\text{-}nH_2O)]$$

where $E(OCS^-\text{-}nH_2O)$ represents the energy of the fully optimized $OCS^-(H_2O)_n$ clusters, $E(OCS\text{-}nH_2O)$ corresponds to the energy of the fully optimized neutral hydrated cluster of the OCS, and $E_s(OCS\text{-}nH_2O)$ is the single-point energy of the neutral hydrated cluster at the equilibrium geometry of the hydrated anionic OCS cluster. Table 4 shows the values of VDE and ADE calculated at the B3LYP, BP86, MP2, as well as CCSD(T) methods with the 6-311++G(d,p) basis set. It is important to note that the VDE and ADE values calculated at the MP2 level of theory are less as compared to the other methods. VDEs of the mono- and dihydrated OCS^- have been estimated experimentally and found to be 2.07 ± 0.07 and 2.53 ± 0.07 eV, respectively. The VDE values of the mono- and dihydrated OCS^- obtained by the B3LYP and BP86 methods are closer to the experimental value. Surprisingly, VDE values for the mono- and dihydrated OCS^- calculated at the MP2 and CCSD(T) levels of theory underestimate it by 25 and 12%, respectively, as compared to the experimental value. The calculated ADE value of the monohydrated OCS^- at the MP2 level of calculation is negative, which is not possible because of its high abundance in experiment. This states that the MP2 level of theory underestimates the value of ADE. Nevertheless, the qualitative trend of the detachment energies is similar for all levels of calculations used in this study. Noticeably, the calculated value of the ADE is less than the VDE at all levels of theory due to the fact that the addition of the electron on the OCS molecule destabilizes it by 13 kcal. Figure 3a represents the change in the detachment energy of the microhydrated OCS^- with respect to the number of water molecules at the BP86/6-311++G(d,p) level of calculation. It can be clearly seen that the value of the detachment energy increases linearly up to the four water molecules, and beyond that, the value is almost constant. This trend of the detachment energy could be either of the core switching of the electron from the OCS moiety to the water network or the completion of the primary solvation shell of the OCS^-.

(c). Vertical and Adiabatic Solvation Energies. The electron detachment process from the anionic clusters includes three steps (Figure 4): (1) the desolvation of anionic species

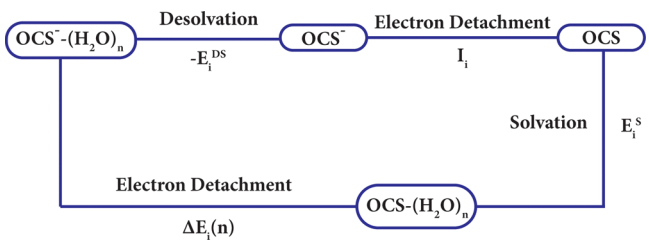

Figure 4. Schematic of the various steps involved in the electron detachment process of the OCS^--$(H_2O)_n$ clusters.

having −1 charge (E_i^{DS}), (2) electron detachment of the ion in the gas phase (I_i^{DE}), and (3) solvation of neutral species (E_i^S). Hence, the sum of all of these energy values equals the detachment energy (ΔE_i^{DE}).

$$[\Delta E_i^{DE}(n)] = I_i^{DE} + E_i^S - E_i^{DS}$$
$$= I_i^{DE} + [\Delta E_i^{SE}(n)]$$

$\Delta E_i^{SE}(n)$ represents the size-dependent solvation energy, and i stand for the vertical or adiabatic. Both the vertical solvation energy (VDSE) and adiabatic solvation energy (ADSE) for the microhydrated OCS^- are calculated at the BP86, B3LYP, MP2, and CCSD(T) levels of theory, and the values are shown in Table 5. The calculated values of the VDSE and ADSE are close to each other and follow a similar trend at all levels of theory. Figure 3b shows the variation of VDSE and ADSE with respect to the number of water molecules of the microhydrated clusters at the BP86/6-311++G(d,p) level of calculation It is evident

DOI: 10.1021/acs.jpca.5b01638
J. Phys. Chem. A 2015, 119, 3644−3652

Table 5. VDSE and ADSE (eV) for the OCS^--$(H_2O)_n$ [n = 1−6] Calculated at the BP86, B3LYP, MP2, and CCSD(T) Methods with the 6-311++G(d,p) Basis Set[a]

	VDSE				ADSE			
	BP86	B3LYP	MP2	CCSD(T)	BP86	B3LYP	MP2	CCSD(T)
OCS^-	1.58	1.67	0.90	1.07	0.17	0.16	−0.57	−0.34
A_{an}	0.68	0.66	0.66	0.65	0.56	0.53	0.55	0.55
B_{an}	1.08	1.02	1.13	1.11	0.84	0.76	0.75	0.75
C_{an}	1.36	1.32	1.36	1.34	0.98	0.94	0.91	0.92
D_{an}	1.73	1.67	1.69	1.68	1.23	1.16	1.19	1.2
E_{an}	1.77	1.70	1.74	1.71	1.20	1.11	1.13	1.08
F_{an}	1.86	1.79	1.84	1.82	1.27	1.21	1.23	1.25

[a]The VDE and ADE of the OCS^- have been depicted at different levels of theory in row one of this table.

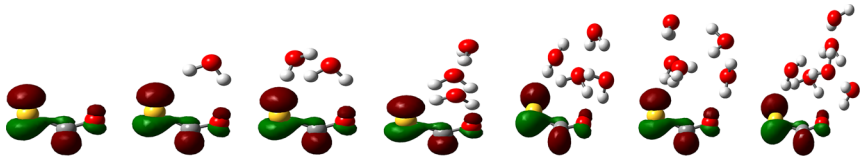

Figure 5. HOMO of the OCS^- monomer as well as its hydrated clusters OCS^--$(H_2O)_n$ (n = 1−6) calculated at the BP86/6-311++G(d,p) level of theory.

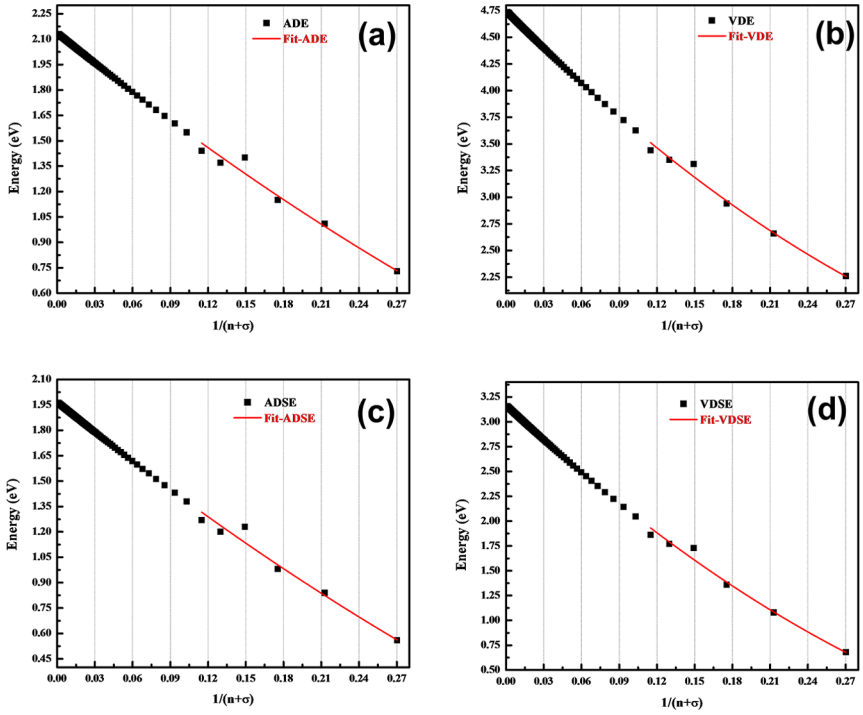

Figure 6. Plot of ΔE(ADE) (a), ΔE(VDE) (b), ΔE(ADSE) (c), and ΔE(VDSE) (d) with respect to the $(n + 2.7)^{-1}$ for the OCS^--$(H_2O)_n$ [n = 1−6] obtained at the BP86/6-311++(d,p) level of calculation. The correlation coefficient for all of the plots is in the range of 0.98−0.99, indicating the reliability of the data.

from the plot that the VDSE and ADSE values increase up to four water molecules and then become constant, similar to the change of the ADE and VDE values.

The trend of the change of detachment (ADE, VDE) and solvation (ADSE, VDSE) energy values with respect to the number of water molecules could be because of either the core switching of the electron from the OCS moiety to the water network or completion of the primary solvation shell of the OCS^-. Figure 5 shows the highest occupied molecular orbital (HOMO) of the OCS^- monomer along with its hydrated cluster of the OCS^- calculated at the BP86/6-311++G (d,p) level of theory. The HOMO for the OCS^- is similar to that of the hydrated OCS^-, clearly demonstrating that the excess electron is intact with OCS^- and that there is no core switching of the electron from the OCS^- to the water cluster. Further weakening of the above logic appears from the comparison of the current VDE data to the data obtained from $(H_2O)_n^-$. If the excess electron is bound to the water network, then the VDE of the system can be calculated by adding the VDE of $(H_2O)_n^-$ and the solvent binding energy of a neutral OCS to a negatively charged cluster. It has been shown that VDE values of the higher $(H_2O)_n^-$ are ∼0.5 eV, [17] and the solvent binding energy

DOI: 10.1021/acs.jpca.5b01638
J. Phys. Chem. A 2015, 119, 3644−3652

of a neutral OCS is a maximum of ∼0.5 eV. Hence, the predicted value of VDE for the microhydrated OCS^- should be ∼1 eV, which is much less as compared to the earlier observed experimental and presently calculated values of VDEs. The energetic and HOMO data suggest that the electrons are intact with the OCS, and there is no core switching upon hydration until six water molecules. A similar conclusion has been drawn for the CO_2^-, which is also metastable in the anionic form and gets stabilized by the hydration.[17] On the basis of this argument, we believe that the trend observed in the dissociation and solvation energies is due to the closing of the primary solvation shell of the OCS^-.

(d). Extrapolation to Bulk. Physical properties such as solvation energy and the detachment energy of the small size hydrated clusters of molecules can be accurately achieved by ab initio calculations; however, they cannot be applied for the larger hydrated clusters due to the demand of the high computational cost. In order to bridge this gap, efforts by various groups have been made to develop a general method by using the existing information on the finite size clusters that can be extrapolated to the infinite size (bulk) clusters. Recently, Pathak et al. developed a generalized microscopic theory to extract the properties of the infinite size clusters including the bulk from the knowledge of the same for finite size clusters.[29,30] The expression of the general equation was given as

$$\Delta E(n) = \Delta E(\infty) + \frac{A}{(n+\sigma)} + \frac{B}{(n+\sigma)^2}$$

Here, $\Delta E(n)$ represents the energy value of the physical parameters like ADE, VDE, and so forth of the hydrated clusters of size n, and $\Delta E(\infty)$ represents the energy for the bulk. A and B are coefficients that are related to the solvent density. The parameter σ is calculated by $\sigma = qV_R$, where q represents the charge and V_R corresponds to the solute to solvent volume ratio. In this expression, σ is introduced to avoid the convergence problem as σ is a positive number and greater than unity, which makes $1/(n+\sigma)$ quite smaller than unity even for small size clusters. This method has been successively used to calculate the accurate bulk values of the VDE and ADE of many anionic systems.[29−31]

Figure 6 shows the variation of the detachment [ADE, VDE (Figure 6a and b)] and solvation [ADSE, VDSE (Figure 6c and d)] energies of the hydrated OCS^- (black points) calculated at the BP86/6-311++G(d,p) level of theory with respect to the $(n+\sigma)^{-1}$, where the σ value for the OCS^- has been found to be 2.7. The data have been fitted to an appropriate equation to find out the optimum values of A and B (red line in Figure 6) and extrapolated to get the bulk values of the detachment and solvation energies. The best fit expression for the ADE, VDE, ADSE, and VDSE are found to be the following

$$\Delta E(\mathrm{ADE}) = \frac{2.99}{(n+2.7)^2} + \frac{6.00}{n+2.7} + 2.13$$

$$\Delta E(\mathrm{VDE}) = \frac{9.94}{(n+2.7)^2} + \frac{11.90}{n+2.7} + 4.74$$

$$\Delta E(\mathrm{ADSE}) = \frac{2.98}{(n+2.7)^2} + \frac{6.01}{n+2.7} + 1.96$$

$$\Delta E(\mathrm{VDSE}) = \frac{9.94}{(n+2.7)^2} + \frac{11.90}{n+2.7} + 3.16$$

The bulk values of the ADE, VDE, ADSE, and VDSE were estimated to be 2.13, 4.74, 1.96, and 3.16 eV, respectively, at the BP86 level of theory by extrapolation using the above-mentioned equations. It is important to mention that the correlation coefficients for all of the plots are in the range of 0.98−0.99, indicating the robustness of the equation used. The same approach has been adopted to obtain the bulk values of ADE, VDE, ADSE, and VDSE at the B3LYP, MP2, and CCSD(T) levels of theory, and the respective values are shown in Table 6. The obtained values of the bulk detachment

Table 6. Bulk Values of the ADE and VDE (eV) as well as ADSE and VDSE (eV) Calculated at the BP86, B3LYP, MP2, and CCSD(T) Methods with the 6-311++G(d,p) Basis Set

	ADE	VDE	ADSE	VDSE
BP86	2.13	4.74	1.96	3.16
B3LYP	2.18	4.80	1.97	3.13
MP2	2.03	3.61	2.30	2.14
CCSD(T)	1.73	3.80	2.36	2.74

energies for the B3LYP and BP86 are close and higher than those of the MP2 and CCSD(T) levels of theory. This is because of the fact that MP2 and CCSD(T) levels of theory underestimate the value of detachment energies of small size hydrated clusters of OCS^-. The predicted bulk value data for the OCS^- could not be validated due to lack of experimental data. However, we believe that the values obtained for the detachment and solvation energies at the BP86 and B3LYP levels of theory are reliable due to the closeness of the VDE data obtained at that level of theory with the experimental data as well as very good correlation coefficients of the fitting. This study depicts that the bulk values of VDE and ADE of the hydrated OCS^- have been increased by the 3.2 and 1.8 eV as compared to the bare OCS^-. In the absence of experimental bulk values of the detachment and solvation energies for this system, the values obtained in this paper may be used in the future for simulation of OCS in the atmosphere.

CONCLUSION

The effect of microhydration on the neutral and anionic OCS has been studied by the B3LYP, BP86, and MP2 methods with the 6-311++G(d,p) basis set. The structure, energetics, and photoelectron spectral properties of the microhydrated OCS as well as OCS^- have been investigated up to six water molecules by using the different levels of methods. OCS is linear in the neutral state, whereas it is bent in the anionic state. Water binds with the OCS through the single hydrogen bond (O−H···O or O−H···S) in the OCS-$(H_2O)_n$ [n = 1−6], whereas a double hydrogen bond (O−H···S and O−H···O) along with a single hydrogen bond stabilizes it to the microhydrated OCS^-. The average stabilization energy increases by 9.5 kcal/mol for microhydrated OCS clusters, whereas it increases by 12.6 kcal/mol for microhydrated OCS^- with successive addition of water. Energy decomposition analysis shows that the electrostatic and the exchange energies are the main contributors to the total stabilization energy of the microhydrated OCS and OCS^- clusters. Both ADE and VDE along with the solvation energies have been calculated at the different levels of theory. It has been observed that B3LYP and BP86 levels of calculations provide ADE and VDE values closer to the experimental one. It has been also observed that the values of the ADE, VDE, ADSE, and VDSE increase up to the fourth water molecule and then

DOI: 10.1021/acs.jpca.5b01638
J. Phys. Chem. A 2015, 119, 3644−3652

become constant. This trend of detachment and solvation energies has been assigned to the completion of the first solvation shell of the OCS^- with four water molecules. Finally, an analytical expression has been used to get the bulk value of the detachment and solvation energies from the existing information on the finite size clusters. The present study reveals that hydration increases the detachment energy of the OCS^- by ~3.2 eV.

■ ASSOCIATED CONTENT

Supporting Information

The energetics of OCS-$(H_2O)_n$ as well as OCS^--$(H_2O)_n$ [n = 1−6], calculated with the MP2, B3LYP, and BP86 methods with the 6-311++G(d,p) basis set are provided. This material is available free of charge via the Internet at http://pubs.acs.org.

■ AUTHOR INFORMATION

Corresponding Author

*E-mail: sppcs@iacs.res.in.

Notes

The authors declare no competing financial interest.

■ ACKNOWLEDGMENTS

This work is supported by the research grant provided by the council of scientific and industrial research [Grant No. 01(2803)/14/EMR-II] India. S.M. thanks IACS for the fellowship. We thank Dr. S. Bhattacharya for critical comments and Abha Bhattacharya for careful reading of the manuscript.

■ REFERENCES

(1) Kesselmeier, J.; Hubert, A. Exchange of reduced volatile sulfur compounds between leaf litter and the atmosphere. *Atmos. Environ.* **2002**, *36*, 4679−4686.

(2) Ferm, R. J. The chemistry of carbonyl sulfide. *Chem. Rev.* **1957**, *57*, 621−640.

(3) Svoronos, P. D. N.; Bruno, T. J. Carbonyl Sulfide: A review of its chemistry and properties. *Ind. Eng. Chem. Res.* **2002**, *41*, 5321−5336.

(4) Wójcik, M. J.; Boczar, M.; Ford, T. A. Ab initio study of energies, structures and vibrational spectra of the complexes of water with carbon oxysulfide and nitrous oxide. *Chem. Phys. Lett.* **2001**, *348*, 126−130.

(5) Deng, C.; Li, Q.-G.; Ren, Y.; Wong, N.-B.; Chu, S.-Y.; Zhu, H.-J. A comprehensive theoretical study on the hydrolysis of carbonyl sulfide in the neutral water. *J. Comput. Chem.* **2008**, *29*, 466−480.

(6) Hartt, G. M.; Shields, G. C.; Kirschner, K. N. Hydration of OCS with one to four water molecules in atmospheric and laboratory conditions. *J. Phys. Chem. A* **2008**, *112*, 4490−4495.

(7) Morrell, T. E.; Shields, G. C. Atmospheric implications for formation of clusters of ammonium and 1−10 water molecules. *J. Phys. Chem. A* **2010**, *114*, 4266−4271.

(8) Tatamitani, Y.; Ogata, T. Microwave Fourier transform spectrum of the water-carbonyl sulfide complex. *J. Chem. Phys.* **2004**, *121*, 9885−9890.

(9) Surber, E.; Ananthavel, S. P.; Sanov, A. Nonexistent electron affinity of OCS and the stabilization of carbonyl sulfide anions by gas phase hydration. *J. Chem. Phys.* **2002**, *116*, 1920−1929.

(10) Surber, E.; Sanov, A. Photoelectron imaging spectroscopy of molecular and cluster anions: CS_2^- and $OCS^-(H_2O)_{1,2}$. *J. Chem. Phys.* **2002**, *116*, 5921−5924.

(11) Surber, E.; Sanov, A. Photoelectron imaging of carbonyl sulfide cluster anions: Isomer coexistence and competition of excited-state decay mechanisms. *J. Chem. Phys.* **2003**, *118*, 9192−9200.

(12) Asmis, K. R.; Neumark, D. M. Vibrational Spectroscopy of microhydrated conjugate base anions. *Acc. Chem. Res.* **2011**, *45*, 43−52.

(13) Cabarcos, O. M.; Weinheimer, C. J.; Lisy, J. M.; Xantheas, S. S. Microscopic hydration of the fluoride anion. *J. Chem. Phys.* **1999**, *110*, 5−8.

(14) Majumdar, D.; Kim, J.; Kim, K. S. Charge transfer to solvent (CTTS) energies of small $X^-(H_2O)_{n=1-4}$ (X = F, Cl, Br, I) clusters: Ab initio study. *J. Chem. Phys.* **2000**, *112*, 101−105.

(15) Robertson, W. H.; Diken, E. G.; Price, E. A.; Shin, J.-W.; Johnson, M. A. Spectroscopic determination of the OH^- solvation shell in the $OH^-\cdot(H_2O)_n$ clusters. *Science* **2003**, *299*, 1367−1371.

(16) Robertson, W. H.; Price, E. A.; Weber, J. M.; Shin, J.-W.; Weddle, G. H.; Johnson, M. A. Infrared signatures of a water molecule attached to triatomic domains of molecular Anions: Evolution of the H-bonding configuration with domain length. *J. Phys. Chem. A* **2003**, *107*, 6527−6532.

(17) Saeki, M.; Tsukuda, T.; Iwata, S.; Nagata, T. Electronic isomers in $[(CO_2)_nROH]^-$ cluster anions. II. Ab initio calculations. *J. Chem. Phys.* **1999**, *111*, 6333−6344.

(18) Schneider, H.; Weber, J. M. Infrared spectra of $SF_6^-\cdot(H_2O)_n$ (n = 1−3): Incipient reaction and delayed onset of water network formation. *J. Chem. Phys.* **2007**, *127*, 174302/1−174302/10.

(19) Wang, X.-B.; Wang, L.-S. Photoelectron spectroscopy of multiply charged anions. *Annu. Rev. Phys. Chem.* **2009**, *60*, 105−126.

(20) Woronowicz, E. A.; Robertson, W. H.; Weddle, G. H.; Johnson, M. A.; Myshakin, E. M.; Jordan, K. D. Infrared spectroscopic characterization of the symmetrical hydration motif in the $SO_2^-\cdot H_2O$ Complex. *J. Phys. Chem. A* **2002**, *106*, 7086−7089.

(21) Yacovitch, T. I.; Wende, T.; Jiang, L.; Heine, N.; Meijer, G.; Neumark, D. M.; Asmis, K. R. Infrared spectroscopy of hydrated bisulfate anion clusters: $HSO_4^-(H_2O)_{1-16}$. *J. Phys. Chem. Lett.* **2011**, *2*, 2135−2140.

(22) Sheps, L.; Miller, E. M.; Horvath, S.; Thompson, M. A.; Parson, R.; McCoy, A. B.; Lineberger, W. C. Solvent-mediated charge redistribution in photodissociation of IBr^- and $IBr^-(CO_2)$. *J. Chem. Phys.* **2011**, *134*, 184311/1−184311/9.

(23) Frisch, M. J.; Trucks, G. W.; Schlegel, H. B.; Scuseria, G. E.; Robb, M. A.; Cheeseman, J. R.; Scalmani, G.; Barone, V.; Mennucci, B.; Petersson, G. A; et al. *Gaussian 09*, revision B.01; Gaussian, Inc.: Wallingford, CT, 2010.

(24) Schmidt, M. W.; Baldridge, K. K.; Boatz, J. A.; Elbert, S. T.; Gordon, M. S.; Jensen, J. H.; Koseki, S.; Matsunaga, N.; Nguyen, K. A.; Su, S.; et al. General atomic and molecular electronic structure system. *J. Comput. Chem.* **1993**, *14*, 1347−1363.

(25) Hammond, J. R.; Govind, N.; Kowalski, K.; Autschbach, J.; Xantheas, S. S. Accurate dipole polarizabilities for water clusters n = 2−12 at the coupled-cluster level of theory and benchmarking of various density functionals. *J. Chem. Phys.* **2009**, *131*, 214103/1−214103/9.

(26) Miliordos, E.; Aprà, E.; Xantheas, S. S. Optimal geometries and harmonic vibrational frequencies of the global minima of water clusters and several hexamer local minima at the CCSD(T) level of theory. *J. Chem. Phys.* **2013**, *139*, 114302/1−114302/13.

(27) Zhan, C.-G.; Dixon, D. A. First-principles determination of the absolute hydration free energy of the hydroxide ion. *J. Phys. Chem. A* **2002**, *106*, 9737−9744.

(28) Zhan, C.-G.; Dixon, D. A. Hydration of the fluoride anion: Structures and absolute hydration free energy from first-principles electronic structure calculations. *J. Phys. Chem. A* **2004**, *108*, 2020−2029.

(29) Pathak, A. K.; Samanta, A. K.; Maity, D. K.; Mukherjee, T.; Ghosh, S. K. Generalized microscopic theory for the detachment energy of solvated negatively charged ions in finite size clusters: A Step toward Bulk. *J. Phys. Chem. Lett.* **2010**, *1*, 886−890.

(30) Pathak, A. K.; Samanta, A. K.; Maity, D. K.; Mukherjee, T.; Ghosh, S. K. Instability range of microsolvated multiply charged negative ions: Prediction from detachment energy of stable hydrated clusters. *Phys. Rev. E* **2011**, *83*, 021112/1−02112/5.

(31) Pathak, A. K. A theoretical study on structures, energetics, and spectra of $Br^-\cdot nCO_2$ clusters: Towards bridging the gap between

DOI: 10.1021/acs.jpca.5b01638
J. Phys. Chem. A 2015, 119, 3644−3652

micro-domain and macro-domain. *J. Chem. Phys.* **2012**, *136*, 234306/1−23306/7.

DOI: 10.1021/acs.jpca.5b01638
J. Phys. Chem. A 2015, 119, 3644−3652